

We are IntechOpen, the world's leading publisher of Open Access books Built by scientists, for scientists

6,900

Open access books available

186,000

International authors and editors

200M

Downloads

Our authors are among the

154

Countries delivered to

TOP 1%

most cited scientists

12.2%

Contributors from top 500 universities



WEB OF SCIENCE™

Selection of our books indexed in the Book Citation Index
in Web of Science™ Core Collection (BKCI)

Interested in publishing with us?
Contact book.department@intechopen.com

Numbers displayed above are based on latest data collected.
For more information visit www.intechopen.com



Sophisticated Biomedical Tissue Measurement Using Image Analysis and Virtual Instrumentation

Libor Hargaš, Dušan Koniar and Stanislav Štofán
*University of Žilina, Faculty of Electrical Engineering,
 Slovakia*

1. Introduction

Modern medical diagnostic and measurement methods are situated in the intersection of conventional science and industry branches: physics, electronics, informatics, telecommunications and medicine. This fact supports mutual cooperation between medical and technical institutes for research purposes.

Some of the last medical conferences which took place in Slovakia and focused on respiratory system diagnostics brought information about missing workstations for cinematic analysis of respiratory epithelium.

In 2009 started European projects Centre of Experimental and Clinical Respiriology I and II, and Measurement of Respiratory Epithelium Cilium Kinematics between Jessenius Medical Faculty in Martin and University of Žilina (both Slovakia). The main goal of these projects is design and verification of experimental workstation with high speed camera linked with light microscope.

From the technical point of view, the most important is that analyzed microscopic objects in motion have high frequency (ca. 18-30 Hz) and they are too small to be equipped with conventional sensors of cinematic parameters. These facts puts accent for conception using means of image signal processing (software tools – virtual instrumentation LabVIEW) and move solution from spatial to frequency (time) domain.

The main topics are frequency measurement and control with high speed video camera and microscope using LabVIEW. The system is designed as phantom and real measurement. Phantom is realized with linear motor and controlled by DSP processor. The motor frequency is measured using image acquisition. This acquisition is done by high speed video camera. The sequences of captured images are processing with image analysis. Image analysis and other algorithms are done by virtual instrumentation using LabVIEW. The parameters of measured objects give relevant information about frequency and trajectory. This system can be used in sophisticated measurements in many educational, research and industrial applications where moving objects of investigation can't be equipped with sensors of cinematic parameters.

2. Structure and function of respiratory epithelium

The human respiratory apparatus is characterized by large surface in continual interaction with outer environment. Many foreign particles are inhaled to this apparatus in the inbreath

phase, but we know some defence mechanisms: surface moisturizing or particles removing by mucociliary transport.

The respiratory mucous membrane is created from glandular epithelium (covering the layer producing mucus) and ciliated epithelium of various types, which moves mucus with foreign particles out of the respiratory apparatus (Jelinek, 2003).

One phase of cilia movement is called effective stroke, when cilia pike (end) shifts mucus in oral direction (out of the respiratory apparatus). In the healthy respiratory epithelium, the movements of cilia are synchronized (in one direction) and the mucus is normally transported. Inherited or obtained defects in cilia structure cause immovability or bad synchronization. These structural changes underlie mucus stagnation and continuous infections of the respiratory apparatus. In case of inherited defects, we can talk about PCD (Primary Ciliary Dyskinesia) syndrome or cystic fibrosis.

Objects investigated by light transmission microscopy usually can't be highlighted using reflection marks or equipped with sensors of kinematics parameters. In this case we often use advantages of image analysis and signal processing. Some methods for frequency measurement (using photodiode and photomultiplier) of biomechanical or microscopic objects can't do the correct analysis of structure pathologies. The most progressive method is high speed digital video method, which brings relatively good results in formation of mathematical and mechanical model of structure movement (Eyman, 2006).

On the other side, optimal light conditions in microscope can be achieved using various types of regulators (dimmers). Quality of obtained and analyzed digital images depends on acquisition system and its settings. Tissue measurement in modern medical praxis needs mutual cooperation of medicine, electronics and signal processing.

As example of moving biomechanical system we can consider cilium of respiratory epithelium cell (Fig. 1). Each ciliated cell of respiratory epithelium contains ca. 200 cilia (6 μm long) beating with frequency up to 30 Hz.

Cilia are synchronized with metachronal waves propagated in periciliary liquid. From the basic position cilium folds down to the epithelium cell (recovery stroke – 75% of beating cycle) and then rapidly darts up to move mucus with its tip (effective stroke) (Javorka, 2001). Relatively high frequency of cilium movement leads to high requirements for the parts of acquisition system – microscope, camera, acquisition computer and others.

3. Currently used methods for CBF (Ciliary Beat Frequency) diagnostics

Ciliated cells are obtained from nose using a cytological brush; after being put into saline, they perform their physiological functions for a short time (max. 20 minutes). Currently, we can investigate the kinetic and structural parameters of cilia by light and electron microscopy. Thanks to good discrimination ability (10-9 m), electron microscopy is used mainly for structural parameters investigation. Light microscopy has smaller discrimination ability (10-6 m) than electron microscopy, but it is a sufficient method for movement analysis; in addition, light microscopy is cheaper and less time-consuming.

There are some advanced methods, such as high-speed cinematography, laser light spectroscopy, photoelectrical measurements and stroboscopy. These methods often need expensive and sophisticated equipment and in many cases cannot reveal the primary cause of dyskinesia. Another problem is frequency analysis: frequency seems to be normal if a significant number of cilia are not damaged.

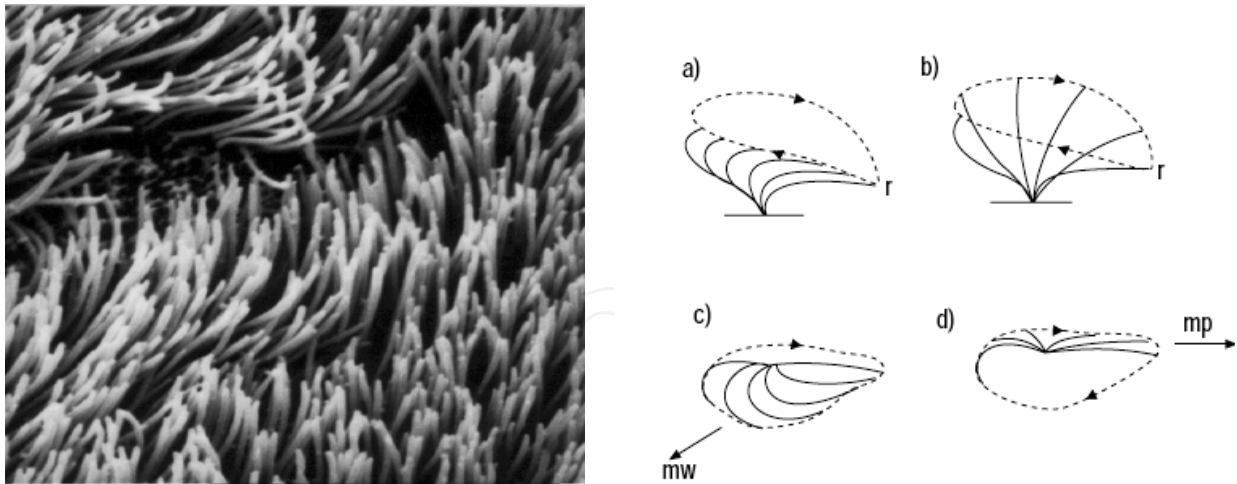


Fig. 1. Ciliated respiratory epithelium in electron microscopy imaging mode and phases of cilia movement

In these days, in clinical praxis, light and electron microscopy are used in many research centres for structure and movement study of biological objects. Electron microscopy has bigger resolution power (1 nm) than light microscopy (1 μm), so we can use it for structure study, but this diagnostics is more expensive. Light microscopy (usually using phase contrast typical for biology measurements) is used for movement study. In case of cilia movement study, there are some sophisticated and expensive methods based on fast and quality hardware components like high speed digital cameras, stroboscopes, photo multipliers and many others. These methods require long time training and we can find them in few research centres in the world. Some methods for frequency measurement (using photodiode and photomultiplier) can't do the correct analysis of object structure pathologies. The most progressive method is high speed digital video method, which brings relatively good results in formation of mathematical and mechanical model of cilia movement (or other biological objects) (Eyman, 2006).

3.1 High speed video method

In this method the motion of object is recorded with high frame ratio (400 FPS or more). High speed sequence is the basic key for analysis of the selected motion and structural parameters of moving objects. Sequence is then processed frame after frame. At the beginning, frequency or object trajectory were measured manually: specialists were counting the number of frames necessary for one object motion cycle and they were doing statistical measurements. High speed video method needs relatively quick memory storage components for its big dataflow. In the time of origin of this method, there was one main aim: to design some algorithms for automated and real-time analysis of movement kinetics. CBF is measured manually by counting of number of frames needed for 1 ciliary cycle or using formula for better accuracy:

$$CBF = \frac{FPS}{N \cdot 10} \tag{1}$$

where FPS is actual frame ratio of sequence, N is number of frames for 10 object movement cycles (Chilvers & O'Callaghan, 2000). High speed record is previewed in slow mode or frame after frame.

3.2 Photodiode and photomultiplier method

Videosequence is viewed on high resolution display (screen). Photosensitive device (diode, multiplier) is placed near the display surface and focused on the area of beating cilium or periodically moving object. The aperture size is ca. 2,2 μm2. Movement of object modifies intensity values in the relevant image region of interest in the place of photosensitive device. Photodiode or multiplier generates voltage signal, which is processed with the tools of spectral analysis, such as FFT (Fast Fourier Transformation) or PSD (Power Spectral Density).

Study (Chilvers & O’Callaghan, 2000) is the first to compare directly two of the most commonly used methods of estimating ciliary beat frequency of respiratory cilia with high speed imaging. The photomultiplier and photodiode techniques recorded ciliary beat frequencies that were significantly slower than those measured using the digital high speed video method.

The limits of agreement for both methods were wide, which confirms that results obtained using the different techniques cannot be used interchangeably. These results emphasise the need for normal reference ranges of ciliary beat frequency to be established for each technique if it is to be used as a diagnostic test for primary ciliary dyskinesia.

4. Tissue measurement design by virtual instrumentation

Frequency of moving object(s) is measured from a waveform that is generated by the variation in grey-level intensity of the phase-contrast image that results from the repetitive motion of object (cilia). Intensity variance curve from high speed video recording is processed using various methods (Zhang & Sanderson, 2003).

The key elements of designed workstation concept are high speed camera and acquisition computer. Camera must have sufficient frame ratio to make analysis more accurate. High frequency of recording specifies usage of powerful computer due to amounts of image data. High frequency also requests higher microscope illumination, which can be adaptive controlled (in spectrum and in intensity). This task belongs to power electronics: to find optimal light source and its topology with suitable type of supply and ability of automatic control.

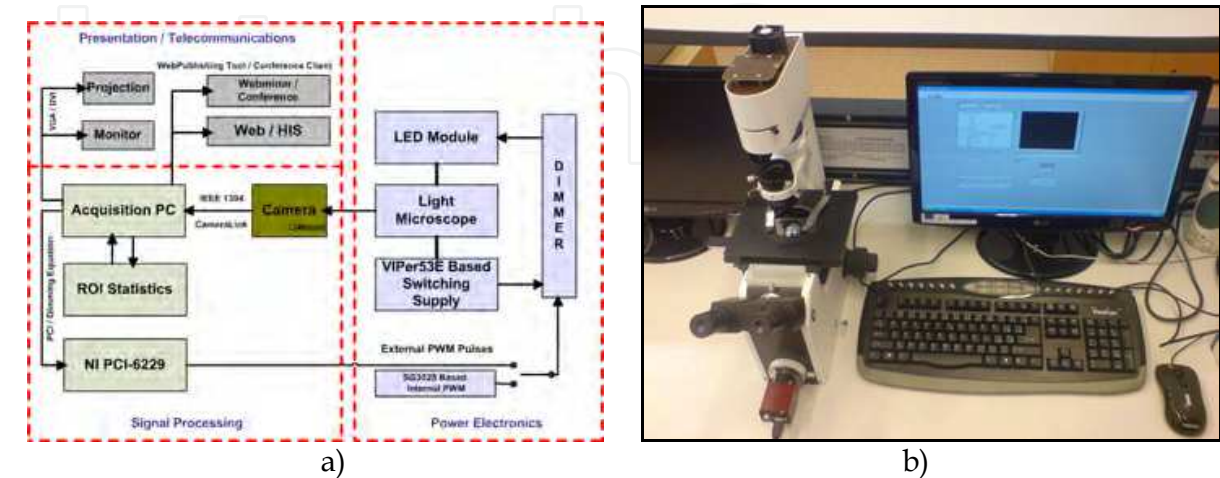


Fig. 2. a) Block diagram of hf (high frequency) video workstation – main components and relations between them, b) Inverse microscope MODEL IM 1C

Recording, preprocessing and analysis of obtained video sequences are done on acquisition computer. Computer communicates with microscope illumination source (this regulation is based on statistical analysis of recorded image). This computer is also connected to the Ethernet / Internet to share analyzed information to secured clinical information systems (HIS). This functionality also enables to control whole experiment through Internet or make “webminars” using conference client.

Some of the main parts of workstation (Fig. 2a) is composed from changeable modules, what creates variability of system. Detailed description and possibility analysis of most important parts is done in the tables in following chapters.

4.1 Videosequence acquisition system

The first real measurements (in Clinic of pathological physiology, Jessenius Faculty of Medicine, Martin, Slovakia) were taken after algorithm debugging on phantoms. Because the ciliary beating frequency ‘in vitro’ goes down from ca. 18 Hz to a half value, primary we used acquisition system with slower camera. In the first approach, we have generated beating frequencies 3 Hz and 9 Hz. Phantoms were recorded with camera AVT Marlin F-046B using 60 FPS recording modes (Fig. 3a). AVT Marlin F-046B camera was connected to inverse biological light microscope MODEL IM 1C via C-mount adaptor. Sequences from camera were stored on acquisition computer through IEEE 1394 (FireWire) as uncompressed sequences with parameters: 8 BPP / 640 x 480 pxl / 60 fps.

In designed system we can use two cameras: AlliedVision AVT Marlin F-046B (60 fps) and Basler A504kc (500+ fps) (Fig. 3b). Both cameras (Fig. 3) are linked directly to microscope via C-Mount or F-to-C-Mount adaptor.



Fig. 3. a) Camera AVT Marlin F-046B, b) Basler A504kc

4.2 Light microscopy

The issue of kinetic analysis of ciliated cells can be divided into few basic steps: image (video) acquisition, image pre-processing, kinetic parameters analysis (frequency and trajectory).

Hardware acquisition equipment is: inverse biological light microscope and monochrome camera connected to PC through IEEE 1394 (FireWire). LabVIEW application is the software platform for videosequence acquisition. The acquisition system and camera connection with microscope are shown in Fig. 2b.

Phase-contrast transmission light microscopy was described by F. Zernik in 1935 for increasing contrast for details in biology objects. Differences in light refraction in the case of constant absorption of light in object are not visible. Phase-contrast method converts phase

difference of transmitted or reflected light waves to intensity difference, which is good visible (Jandoš & Říman & Gemperle, 1985).

Fig. 4a shows light transmission through phase object: this object modifies only the phase, not intensity. Phase contrast then converts $\delta\lambda$ to intensity value.

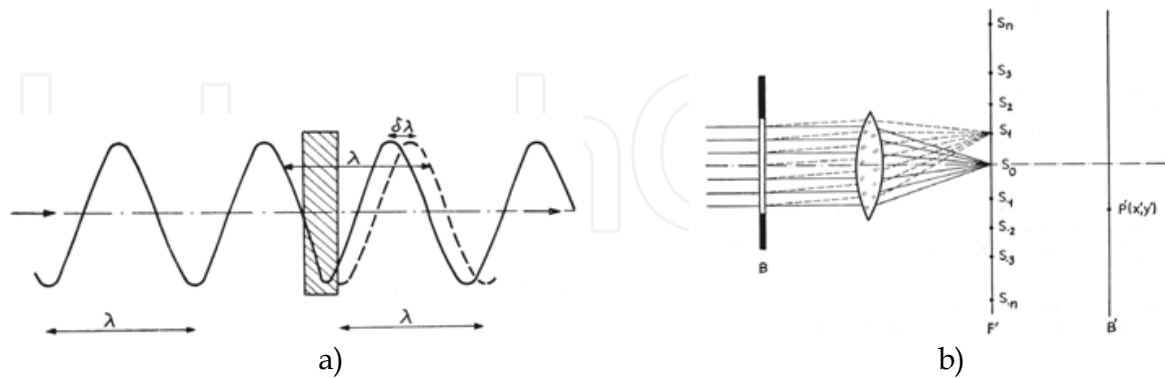


Fig. 4. a) Light transmission through phase object, b) Optical system with diffraction spectrums in focal plane, B - object, F' - focal plane, B' - imaging plane, P'(x';y') - projected point

Abbe's optical theorem says that each object is diffracting, so in the focal plane object creates spectrums from 0-th to N-th order (Fig. 4b.). It is necessary to hold the light from the maximum number of spectrums in the imaging plane for true imaging.

Consider plane light wave with unit amplitude:

$$e^{i2\pi\vec{k}\vec{r}} \tag{2}$$

where \vec{k} is wave vector in the wave direction and $|\vec{k}| = 1/\lambda$; \vec{r} is positional point vector in optical system.

Also consider coordinate system parallel with optical axis of system, then in plane $z = 0$ we can write formula (without object in optical system):

$$V_0(x;y) = e^{i2\pi(k_x \cdot x + k_y \cdot y)} \tag{3}$$

Then relation:

$$F(x;y) = \frac{V(x;y)}{V_0(x;y)} \tag{4}$$

is transfer function of object in optical system. If $F(x;y) \in \mathbb{R}$, then the object is amplitude object (modifies intensity of transmitted light). If $|F(x;y)| = 1$, then the object is phase object, Φ is phase shift and:

$$F(x;y) = e^{i\Phi(x;y)}, \quad \Phi(x;y) \in \mathbb{R}. \tag{5}$$

Intensity of light in $P'(x';y')$ corresponding to point $P(x;y)$ in object (Fig. 4b) in optical imaging system is:

$$I = C2 \cdot |F|^2, \tag{6}$$

where C is characteristic constant of optical system and F is transfer function. In the case of pure phase object and intensity is constant. In the case of weakly phase object $\Phi(x;y) \ll 1$ and we can expand F(x;y) to series with ignoring elements up from 3-th order:

$$F(x;y) = 1 + i\Phi(x;y) \tag{7}$$

The first element of series corresponds to light concentrated in diffraction spectrum of 0-th order and the rest of series corresponds to light from higher order spectrums. We can place phase or absorption plate in the place of 0-th spectrum, which changes the phase of light wave $\pm(\pi/2)$. This plate modifies first element in the series by multiplying it with factor:

$$a.e^{\pm i\frac{\pi}{2}} = \pm ia \tag{8}$$

where a represents absorption ratio. Then the series transforms to:

$$G(x;y) = \pm ia + i\Phi(x;y). \tag{9}$$

Intensity in true imaging is:

$$I = C^2 |G|^2 \approx a^2 \pm 2a\Phi(x;y) \tag{10}$$

if expression $\Phi^2(x;y) \ll 1$ is neglected. Image contrast is then increased and equals:

$$\frac{\pm 2\Phi(x;y)}{a}. \tag{11}$$

Sign “+” in formula for contrast expresses positive contrast: regions with high optical density are bright and placed on dark background. Sign “-” expresses negative contrast, what is inversion of first state.

In practical solution in phase-contrast light microscopes annulus aperture is used. This fact and basic structure of phase-contrast optical system is shown in Fig. 5.

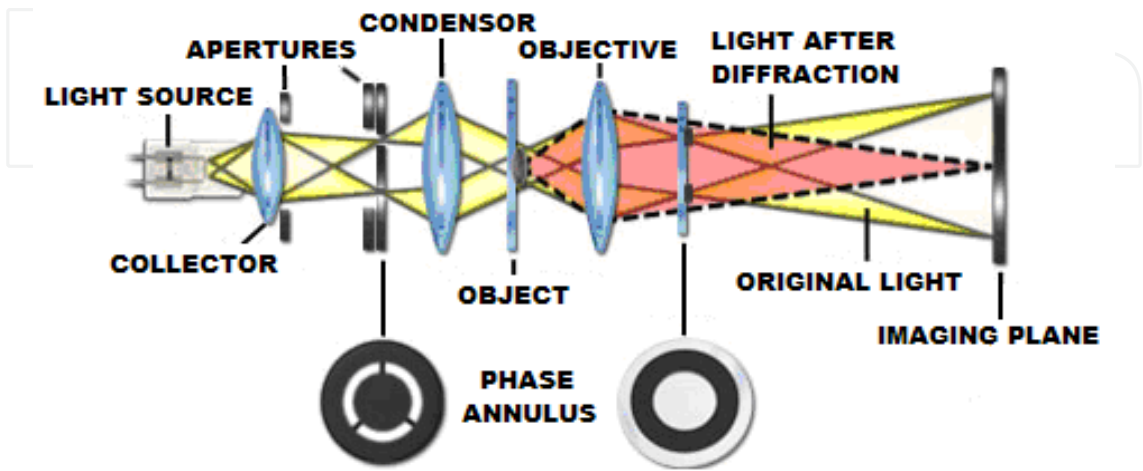


Fig. 5. Structure of phase-contrast light microscopy; position of phase-contrast annulus aperture

4.3 Illumination control by videosequence acquisition process

The reliability of kinematics analysis depends on frame rate of used camera. Higher frame rate (500fps and high) brings more information for analysis but also brings more volume of irrelevant data. Higher frame rate in camera required fast electronic elements used in camera for reading, buffering and data streaming. The reading process from image chip is taken in short time interval. Due to this fact, exposure time is too short, so it is necessary to use lighting source with higher optical (illumination) efficiency.

Our present microscope used as light source the halogen lamp with electrical power 120 watts. The efficiency in this case is very low (10 – 25%). We search the solution, which will provide enough optical power with higher energy efficiency. We have therefore decided to focus on the use of the light source based on LEDs. This group of light sources growth in last time. They have higher energy efficiency, better spectral performance and better geometrical radiating characteristic. The other conditions were a good possibility to the output power control.

It is very important set the illumination conditions by acquisition process and hold their on constant value during all process. We try developing the algorithm that can regulate a soft change of illumination conditions during the acquisition process. The main control loop computes the main value of histogram in current image frame. When has the value changed the algorithm adjusts the change via power regulator of light source.

The block diagram of regulator is on Fig. 6. The flyback converter converts the input voltage from value 230 V AC to 15V DC. It isolates galvanic also the other components. The output current can be maximal 2A. The DC voltage is coming into current source block. The output source is adapted for LED module conditions. We use few variation of value output power (0,1A/0,4A/1A). It is depend on LED module. The current source is based on circuit L200. The output current is switched with MOSFET transistor. The switching is controlled with LabVIEW application. The output power is controlled with change of duty cycle of input PWM signal. The signal is coming from I/O card from computer (for example NI-PCI6229).

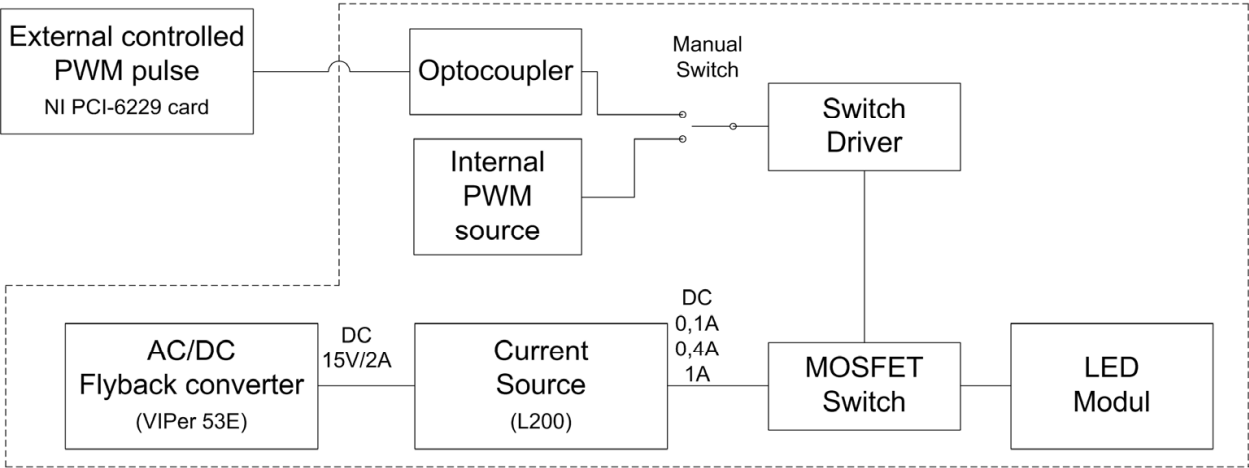


Fig. 6. Illumination regulation block diagram

Fig. 7 shows the illumination dependences on electrical power. The characteristic was measured on LED PG1N-3LXC-SD (ProLight). This LED should replace the previous halogen lamp. It was used in microscope as light source. Now we can take the better energy efficiency (Špánik et. al, 2010).

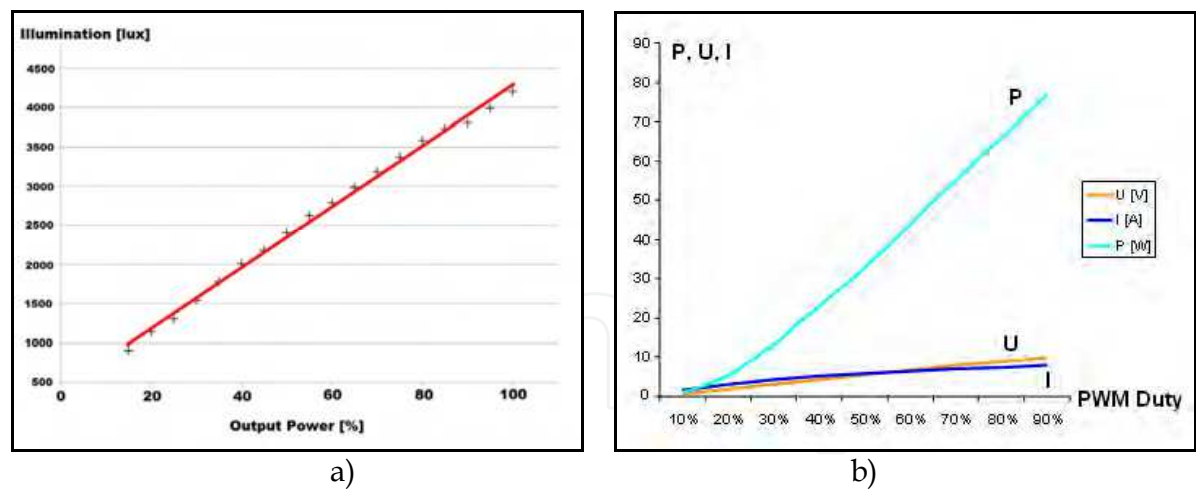


Fig. 7. Illumination dependences on electrical power – a) LED diode, b) halogen lamp

In the case of usage high speed camera system (Basler), microscope illumination is very important. We have changed microscope condenser light source and made some measurements of intensity by Lutron LX-1102 luxmeter. In case of ultra high frame ratio of camera we can meet these essential problems: if the illumination of specimen is too low, frames in video sequence are underexposed and dark; if the illumination of specimen is too high, frames are overexposed and too bright (Fig. 9a-d); high frame ratio causes growth of data for storage, so we must consider optimal connection between camera and acquisition computer. These non-optimal conditions causes same „faults“ in intensity curve. Original maximal value of illumination (measured between condenser optics and specimen) changed from 8,6 klx to ca. 80 klx after replacing 20W halogen lamp for 120W halogen lamp. Heat from condenser must have been removed using active CPU cooler mounted onto microscope or using intelligent dimming tool.

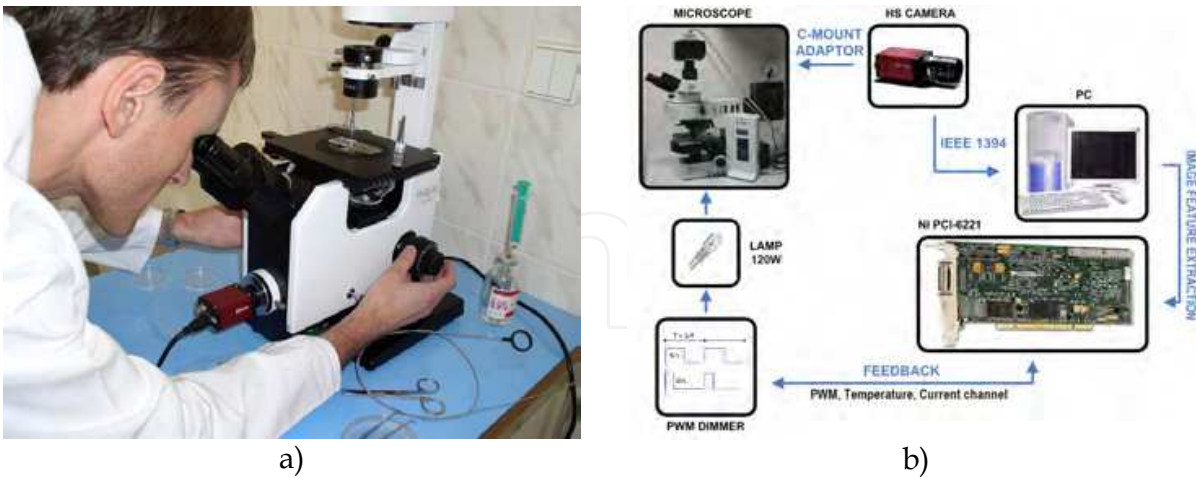


Fig. 8. a) Experimental workstation – microscope connected to digital camera, b) block scheme of whole acquisition scheme –processing

The intelligent dimmer was designed based on simulations. The power supply is made directly from the main supply 230V via input transformer (Frivaldsky et al, 2009). Dimming feature is provided through one PWM channel, which generates driving impulses of switching transistor (Drgoňa et al, 2009). PWM signal is generated in NI PCI-6229 LabVIEW

measurement card and is isolated from power circuit through optocoupler and amplified in transistor driver. PWM has constant frequency of 50 kHz and regulation is done through duty cycle of impulses. This regulation part of acquisition system uses software regulation feedback included in acquisition virtual instrument and will be described later. Power regulation in dependency on duty cycle and its influence on image histogram is shown in Fig. 9e-h.

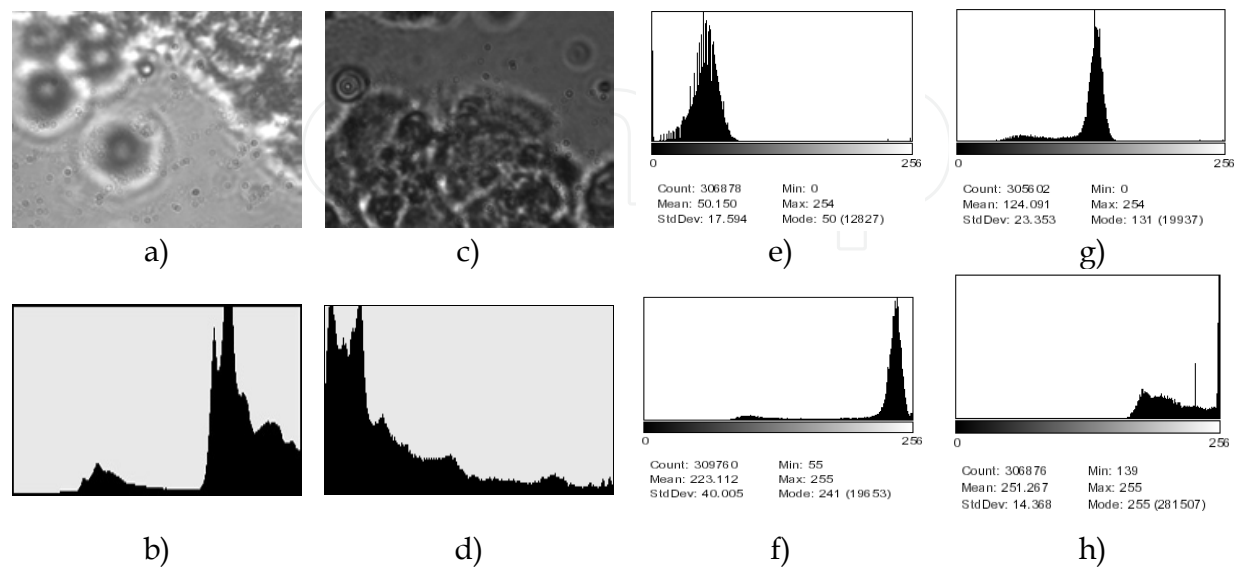


Fig. 9. a) Overexposed image, b) Overexposed image histogram, c) Underexposed image, d) Underexposed image histogram, e) PWM 20%, f) PWM 30%, g) PWM 25%, h) PWM 40%

4.4 Illumination regulation feedback

In process of sequence acquisition, a ROI (Region Of Interest) placed into image extracts important image feature: average image intensity and histogram distribution. Overexposed image has its histogram concentrated to high intensity values and underexposed image to low values (Fig. 9a-d). Histogram distribution is used as regulation parameter for setting up the PWM for halogen lamp dimmer. Dependency of histogram mean (μ) on duty cycle (dc) for actual frame ratio (fps) of video system can be described by kvasi-linear characteristics (Fig. 10).

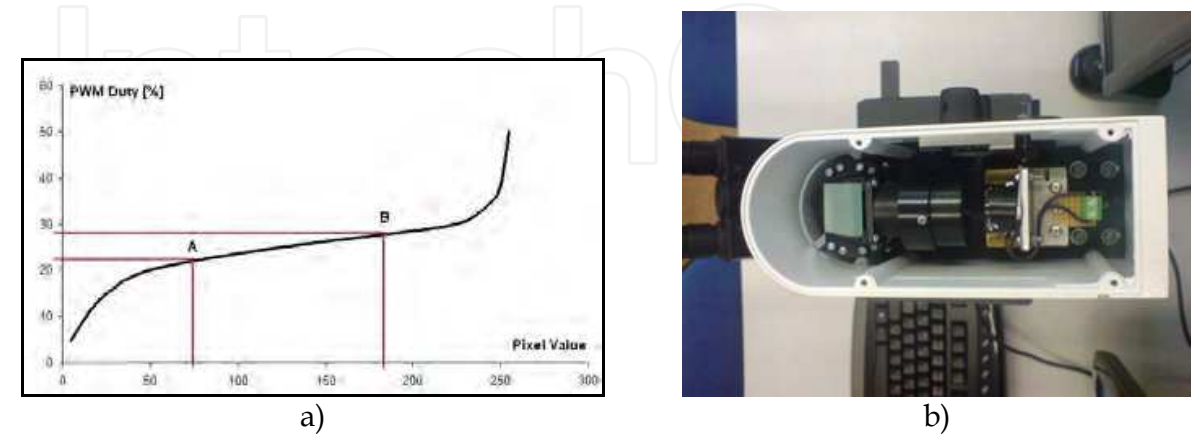


Fig. 10. a) Illumination characteristics for 60 fps framing. Optimal μ_0 corresponds with $d.c_0 = 25\%$. Acceptable duty cycles lies in range 20-30%, all duty cycles under or over this interval brings underexposed or overexposed image, b) microscope illumination module

Regulation algorithm approximates this characteristic with a line using two or more known points:

$$y = ax + b \tag{12}$$

$$A = [\mu_1, dc_1]; B = [\mu_2, dc_2] \tag{13}$$

$$a = \frac{dc_2 - dc_1}{\mu_2 - \mu_1} \tag{14}$$

$$b = dc_1 - \frac{dc_2 - dc_1}{\mu_2 - \mu_1} \mu_1 \tag{15}$$

$$y = \frac{dc_2 - dc_1}{\mu_2 - \mu_1} x + dc_1 - \frac{dc_2 - dc_1}{\mu_2 - \mu_1} \mu_1 \tag{16}$$

and calculates Δdc for setting histogram $\mu_0 \approx 128$, what is half of grayscale range 0 - 255; dc_0 - duty cycle corresponding to μ_0 :

$$\pm \Delta dc = dc_i - dc_0 \tag{17}$$

Delay of the regulation algorithm depends on framing ratio of camera and is 1/fps [s].

5. Analysis and evaluation of videosequence

One of the intensity variance curve analysis methods is described in methods (Zhang & Sanderson, 2003). Researchers from this study saved digital images directly to an array of SCSI (Small Computer System Interface) hard drives configured as a stripped drive; the data storage rate is determined by the speed and number of the individual drives. The data rate is often ca. 120 MB/s.

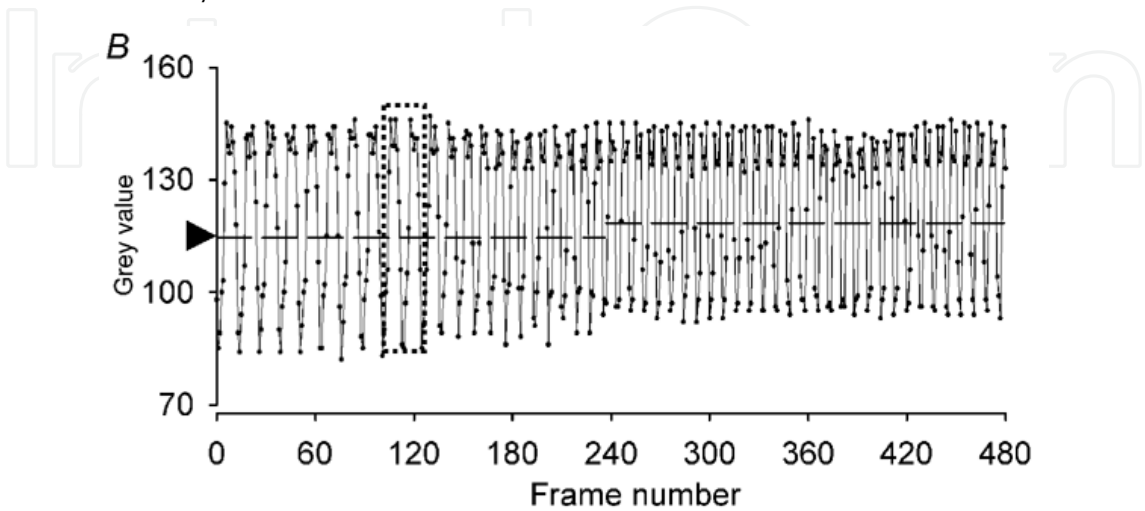


Fig. 11. Intensity variance curve with highlighted beating cycle

Basic problem is to select suitable ROI (Region Of Interest) in image. The best placement is in the end of beating object. Size of ROI underlies optimal signal-to-noise ratio. Researchers from methods (Zhang & Sanderson, 2003) used ROI ca. 3x3 pixels (0,87μm x 0,80μm gap of photo sensitive device).

Fig. 11 shows example of intensity variance curve generated by photo sensitive device captured from oscilloscope and normalized for 8 BPP grayscale image palette.

Used technique computes object beating frequency by searching points of intersection with “threshold line”. This helps us to indicate starts and ends of each beating cycle. For more accuracy, this technique recalculates analysis parameters after each second.

Consider intensity variance curve like discrete function $G(n)$ (Fig. 12a), where time quantization is done by FPS. For each second we can compute arithmetic mean value of $G(n)$ and call it G_{cross} :

$$G_{cross} = \frac{1}{N} \sum_n G(n),$$

(18)

where N is number of frames for 1 second of recording ($N = FPS$).

Algorithm searches time between two frames F_n and F_{n+1} , where F_n is frame when $G(n) < G_{cross}$ and F_{n+1} is frame when $G(n) > G_{cross}$. This time expresses beating period of periodical motion.

In consequence of noise processes, we can check intersection with G for more than 2 points: $G(n) < G(n+1) < G_{cross} < G(n+2) < G(n+3)$.

Because the intensity variance curve is discrete, accurate intersection time T_{cross} (Fig. 12b) usually lies between two discrete frame times. Providing intensity variance function linear and continuous, we can interpolate T_{cross} with formula:

$$T_{cross} = \frac{F_n + \frac{G_{cross} - G(n)}{G(n+1) - G(n)}}{FPS}$$

(19)

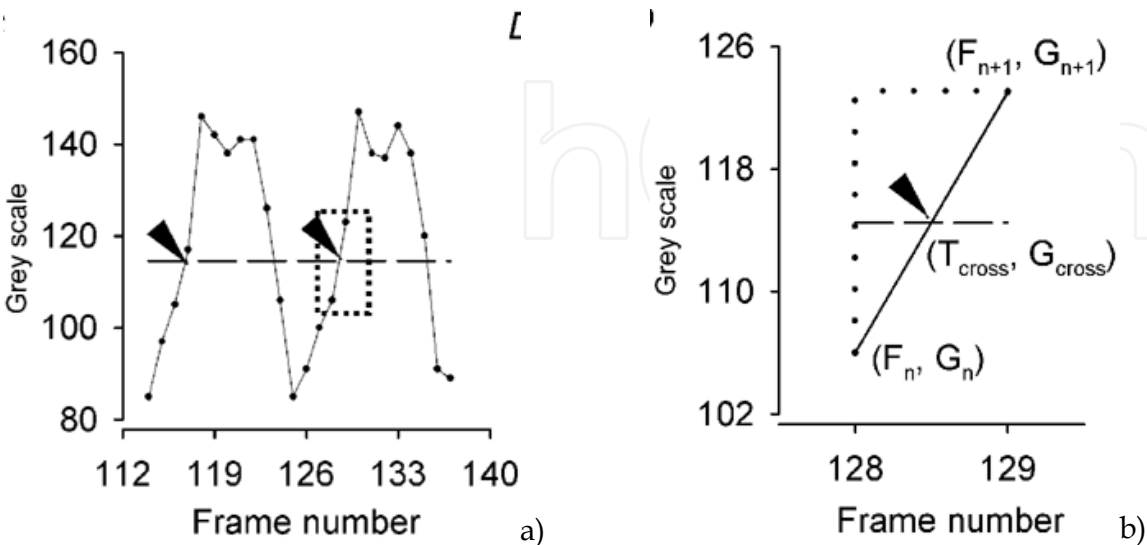


Fig. 12. Object beating cycle; a) starting intersections of each cycle; b) computing of the cross time

5.1 Videosequence preprocessing

Preprocessing has two goals: to shorten analysis time and improve kinetic parameters analysis. Grayscale videosequences are sufficient for further analysis as many LabVIEW tools are applicable only on grayscale image. The given acquisition system can be easily built in medical or laboratory environment. In order to test the applications for sequence pre-processing and kinetic parameters analysis some phantom sequences were acquired (without microscope or using microscope – microscopic grid movement).

Fundamental function for image (videosequence) acquisition is LabVIEW express function for communication with the device on IEEE 1394 port and control items enabling to set up the camera shutter, format, FPS, brightness and gain, number of frames (sequence length). Final videosequence is written as raw video file (*.avi) (Fig. 13a).

The time needed for analysis can be reduced by cutting off of the regions or frames (redundant time intervals) which do not contain relevant information. In this aspect we can talk about time reduction (e.g. frames selection from 7 to 153 of the whole sequence) or spatial reduction (selection of ROI containing isolated cell). Script is very simple and its output is time or spatial (or both) reduced videosequence.

An important phase is improving intensity levels in the whole image. Fig. 13b shows the Front Panel of application for image (sequence) pre-processing. After videosequence opening the following operators and tools can be applied:

- extraction of single color plane,
- lookup Table (LuT) operators,
- convolution (spatial) filtering,
- equalization,
- histogram.

The pre-processing application has many degrees of freedom for user. Filters and tools can be fully combined, so the application can be used in various cases. After the pre-processing phase, the kinetic parameters are analyzed.

- *Extraction of single color plane* - this tool extracts 8-bit gray plane from color image, because many LabVIEW tools and operators work only with grayscale images. The most important is Luminance 8-bit plane (from HSL model, which is RGB derivate). Luminance plane contains information about objects position and minimizes information stored in textures, which is more important for movement detection.
- *Lookup Table (LuT) operators* - Lookup Table is a transfer characteristic (linear, linear in parts, nonlinear) between an original image and a processed image. They enhance and improve intensity relations in the whole image, change brightness and contrast. The kind of LuT operator is BCG Correction. The Lookup exponent is the variable which gives the final curving of the base curve. LuT range is intensity interval on which the LuT curve is applied. While often effective, employing a lookup table may nevertheless result in a severe penalty if the computation that the LUT replaces is relatively simple. Memory retrieval time and the complexity of memory requirements can increase application operation time and system complexity relative to what would be required by straight formula computation. The possibility of polluting the cache may also become a problem.
- *Convolution (spatial) filtering* - convolution filtering belongs to linear filtering. Filter uses a kernel. Kernel moves through the image, convolution between original image and kernel array is calculated on each position and result is written on the central pixel position. Result can be divided with normalization factor N, which is the sum of kernel values or 1.

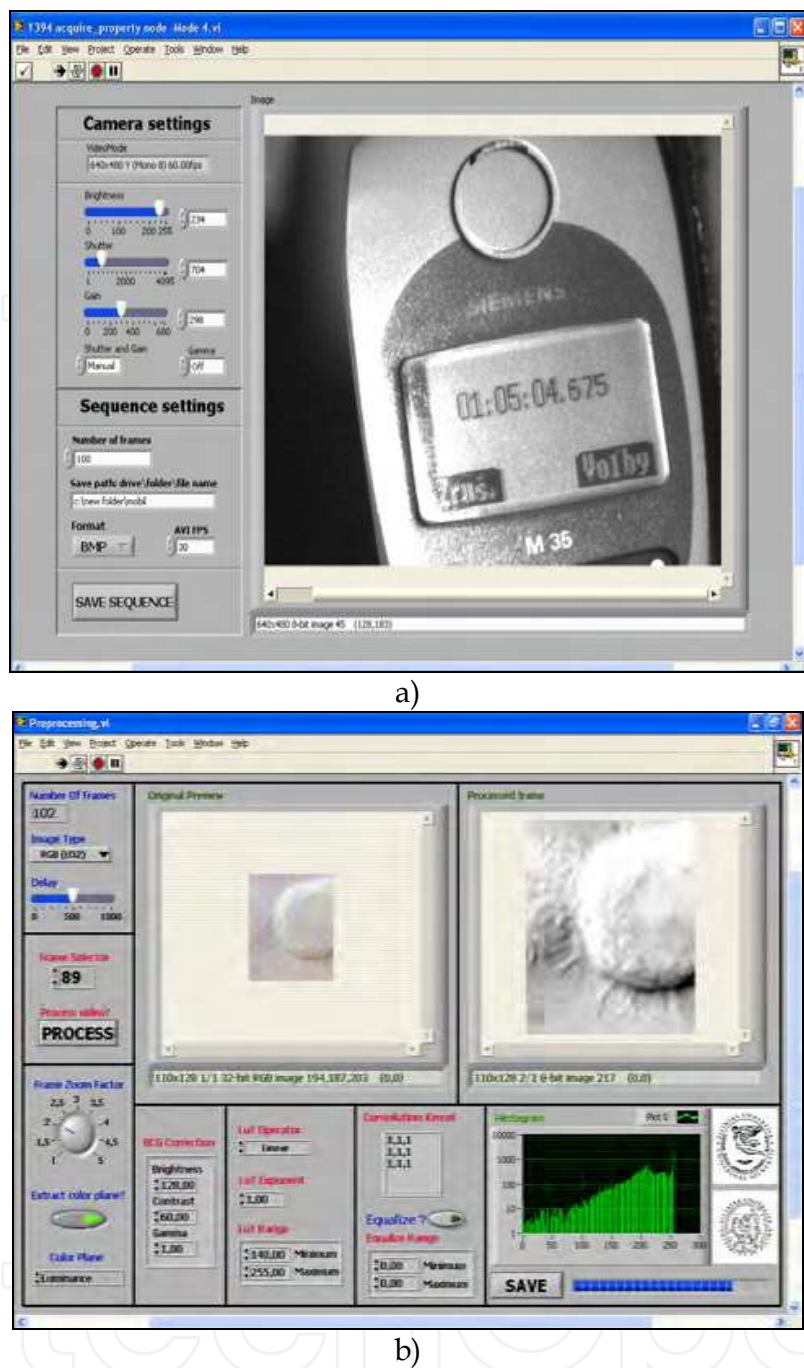


Fig. 13. a) Acquisition application Front Panel, b) Pre-processing application Front Panel - videosequence pre-processing

- *Equalization* - equalization enhances pixel intensities. Equalization range is the value interval on which the transformation is done; this interval will be remapped on 0-255 interval, so we can reveal details from this interval only.
- Consider a discrete grayscale image {x} and let n_i be the number of occurrences of gray level i . The probability of an occurrence of a pixel of level i is:

$$p_x(i) = p_x(x = i) = \frac{n_i}{n}, 0 \leq i < L$$

(20)

L being the total number of gray levels in the image, n being the total number of pixels in the image, and $p_x(i)$ being in fact the image's histogram for pixel value i , normalized to $[0,1]$. Let us also define the cumulative distribution function corresponding to p_x as

$$cdf_x(i) = \sum_{j=0}^i p_x(j) \quad (21)$$

which is also the image's accumulated normalized histogram.

We would like to create a transformation of the form $y = T(x)$ to produce a new image $\{y\}$, such that its CDF will be linearized across the value range, i.e.

$$cdf_x(i) = iK \quad (22)$$

for some constant K . The properties of the CDF allow us to perform such a transform, it is defined as

$$y = T(x) = cdf_x(x) \quad (23)$$

Notice that the T maps the levels into the range $[0,1]$. In order to map the values back into their original range, the following simple transformation needs to be applied on the result:

$$y' = y \cdot (\max\{x\} - \min\{x\}) + \min\{x\} \quad (24)$$

In the case, that the cdf must be normalized to $[0,255]$, the general histogram equalization formula is:

$$h(v) = \text{round} \left(\frac{cdf(v) - cdf_{\min}}{(M \times N) - cdf_{\min}} \times (L - 1) \right) \quad (25)$$

where cdf_{\min} is the minimum value of the cumulative distribution function (in this case 1), $M \times N$ gives the image's number of pixels and L is the number of grey levels used (in most cases, 256).

- *Histogram* - histogram shows the dependency between intensity value and number of pixels of this gray value. Histogram gives us the complex view on the image and facilitates us the noise removal or segmentation.

In a more general mathematical sense, a histogram is a function m_i that counts the number of observations that fall into each of the disjoint categories (known as bins), whereas the graph of a histogram is merely one way to represent a histogram. Thus, if we let n be the total number of observations and k be the total number of bins, the histogram m_i meets the following conditions:

$$n = \sum_{i=1}^k m_i \quad (26)$$

Cumulative histogram - a cumulative histogram is a mapping that counts the cumulative number of observations in all of the bins up to the specified bin. That is, the cumulative histogram M_i of a histogram m_j is defined as:

$$M_i = \sum_{j=1}^i m_j$$

(27)

Number of bins and width – There is no "best" number of bins, and different bin sizes can reveal different features of the data. Some theoreticians have attempted to determine an optimal number of bins, but these methods generally make strong assumptions about the shape of the distribution. The number of bins k can be assigned directly or can be calculated from a suggested bin width h as:

$$k = \left\lceil \frac{\max x - \min x}{h} \right\rceil$$

(28)

The braces indicate the ceiling function.
The preprocessing application has many degrees of freedom for user, filters and tools can be fully combined, so application can be used in various cases. The kinetic parameters are analyzed.

5.2 Phantom acquisition system design

Measurement method designed by our team is based on frequency analysis of intensity variance curve. This curve is obtained from video sequence by capturing intensity variation in selected region of interest (ROI). Curve is then analyzed with FFT algorithm, measurement is verified using curve thresholding and envelope analysis. Whole algorithm is shown in Fig. 14.

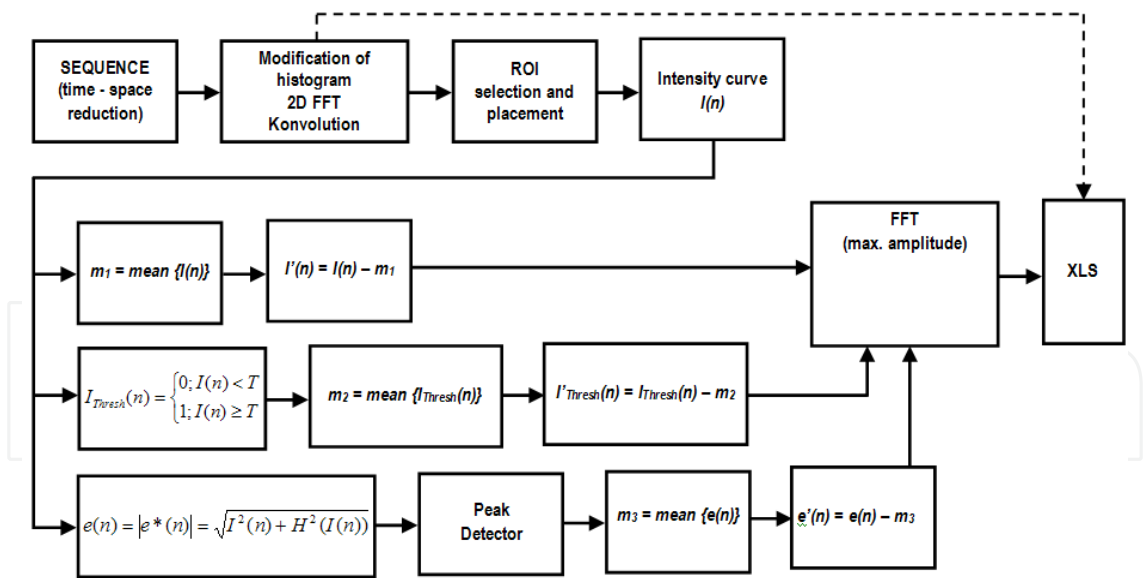


Fig. 14. Frequency measurement algorithm

Measurement is done in graphical development system NI LabVIEW as virtual instrument and results are written as Microsoft Excel XLS file. This component helps to integrate results of investigation to laboratory or clinic information systems. Next advantage of LabVIEW virtual instrument is called Web Publishing Tool. Using this tool we can provide control of whole application through Internet.

To generate an accurate object beating frequency, we used DSP controlled stepping motor with reflection mark on the vane of its propeller (Fig. 15a). Phantoms with defined parameters are common and useful parts in design process of new diagnostic or measuring method.

5.3 Recording of intensity variance curve

On reference frame of videosequence we can interactively select ROI (region of interest) which contains beating object (Fig. 15b). Consider ROI size $k \times l$ pixels with left top corner coordinates $(L;T)$. Then mean intensity value for ROI for N -th frame is:

$$I_{avg}(N) = \frac{1}{k \cdot l} \sum_{i=1}^k \sum_{j=1}^l f(i+T; j+L)_N \quad (29)$$

where $f(i;j)_N$ is intensity value of pixel $(i;j)$ in ROI. Formula (29) is 2-D transformation of (18). Algorithm then creates intensity variance curve from each mean value for all frames. Basic curve is then relation between intensity means and number of frame. If FPS of videosequence is known, we must transform frame axis to time axis using transformation formula:

$$t[\text{sec.}] = \frac{N}{FPS}. \quad (30)$$

Size of ROI underlies the shape of main repetitive pattern of intensity variance curve. Smaller ROIs are more sensible for intensity variance and the curve pattern have bigger differences between maximum and minimum value. On the other hand, bigger ROIs have better “signal-to-noise ratio”.

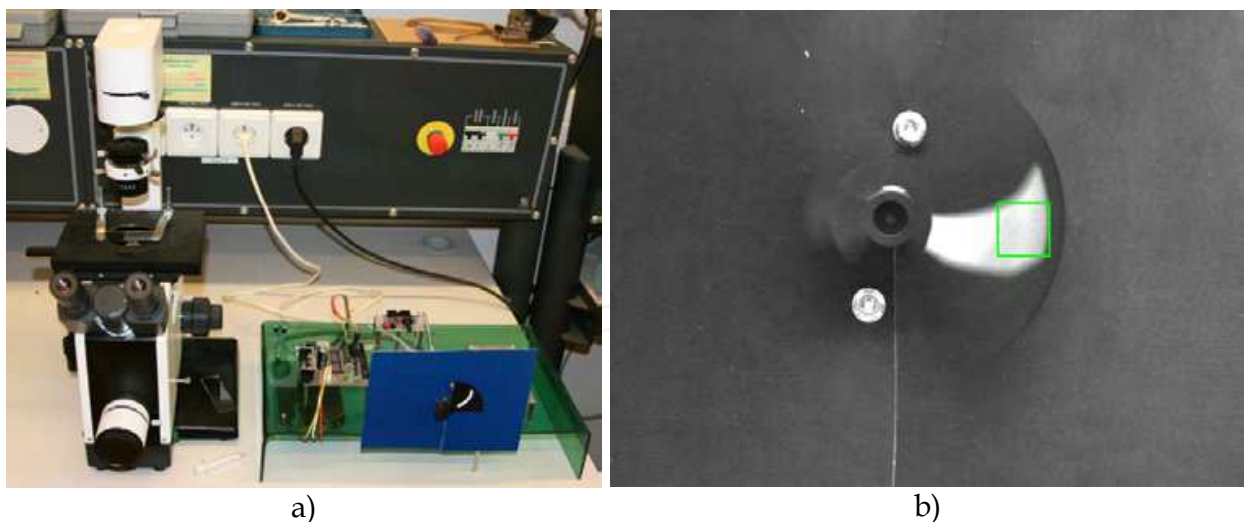


Fig. 15. a) Generator of accurate object beating frequency, b) Frame from phantom videosequence with selected ROI

Curve fineness depends on FPS and used video compressor. Next measurements were taken on raw (uncompressed) AVI file with 60 FPS. Each frame is grayscale bitmap with 8 BPP depth.

In the case of rotating phantom (whole circle or partial circle movement) measured beating frequency would not depend on the ROI placement on the object (base, middle part or end),

because angle speed of object isn't a function of distance from the axis of rotation. Even though (Zhang & Sanderson, 2003) recommends placement of ROI on the end of object, because in the case of cilia, base is joint with epithelial cell and cilia spike movement is relevant part for frequency analysis.

Measurements 1-4 (Fig. 16 and Fig. 17) confirm facts above. ROI size in measurement 1 and 2 influences value differences in beat pattern. Placement of ROI to the base or to the end of object gives equivalent results.

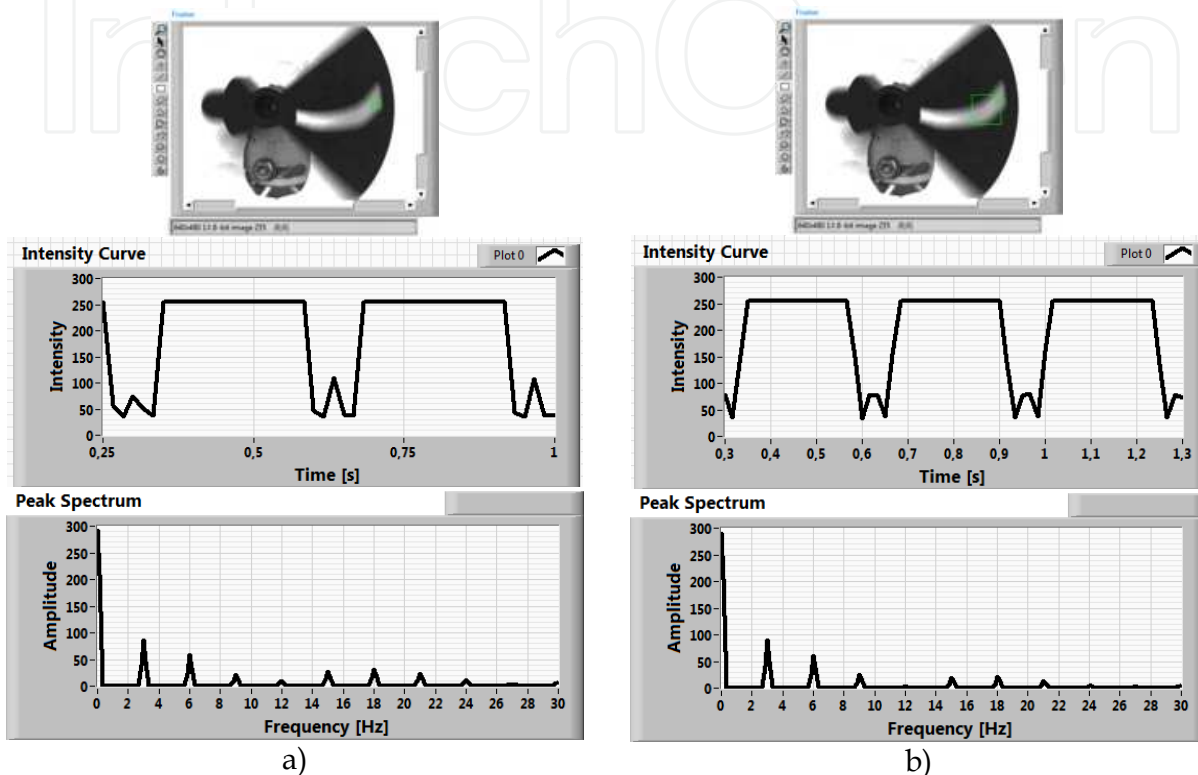


Fig. 16. a) Measurement 1: 3 Hz / ROI size: 15 x 15 (px) / bright background, b) Measurement 2: 3 Hz / ROI size 45 x 45 (px) / bright background

In the case when (FPS/BF) is integral number, we can't see any "floating" in variance curve, because the number of frames needed for one beating cycle of object is integral number too (Fig. 18a). In measurement 1 and 2 the contribution:

$$\frac{FPS}{BF} = \frac{60}{3} = 20 \quad (31)$$

is integral number.

In the measurement 3 and 4, this contribution is $60/9 = 6,67$, what isn't integral number and we can see floating of variance curve (Fig. 18b). This floating is caused by fact that number of frames needed for one beating cycle isn't an integral number.

The more efficient and quick way to do spectral analysis of variance curve is FFT (Fast Fourier Transform). FFT decomposes a sequence of values into components of different frequencies. For discrete signal FFT uses formula (Brigham, 1988):

$$X_k = \sum_{n=0}^{N-1} x(n) \cdot e^{-i2\pi k \frac{n}{N}} \quad (32)$$

where X_k is complex spectral component, $k = 0, \dots, N-1$, $x(n)$ is element of discrete function, N is number of samples used for computing, $N = 2^m$, m is integral number. Computed spectral components are complex number, we can split this complex spectrum to magnitude spectrum (amplitudes) and phase spectrum.

Detailed description of variance curve from measurement 3 and 4 is shown in Fig. 19a. Applying this signal processing tool on variance curve, we can create spectrum and plot it into the spectral graph (Fig. 19b, Fig. 20b). Beating pattern in the curve creates the main spectral component: first harmonic component with maximal peak (amplitude). Because the mean value of intensity curve isn't zero, in the spectrum we can see DC component (in the position of 0 Hz). DC component does not contain any information about object movement, so we can reject it.

5.4 Measurement of frequency (CBF)

Healthy cilia make continuous and synchronized moves. The frequency is often called CBF (Cilia Beat Frequency). This parameter can be measured using the intensity method. In this method, the ROI is created in near surrounding of beating cilia. Passing of cilia across the ROI causes intensity variations in it. The average ROI intensity is recording in time and this periodical curve is processed with tools of frequency analysis. The frequency spectrum of beating can be displayed by application of FFT (Fast Fourier Transform). The PSD graph (Power Spectral Density) can be also displayed, which is FFT of curve autocorrelation. In Fig. 20a is shown graph of intensity variations and in Fig. 20b PSD of this curve. We can also see (Fig. 20b) that Measured frequency is in the range of 17 – 20 Hz and this fact is shown in Fig. 20b. This measured frequency is the physiological value.

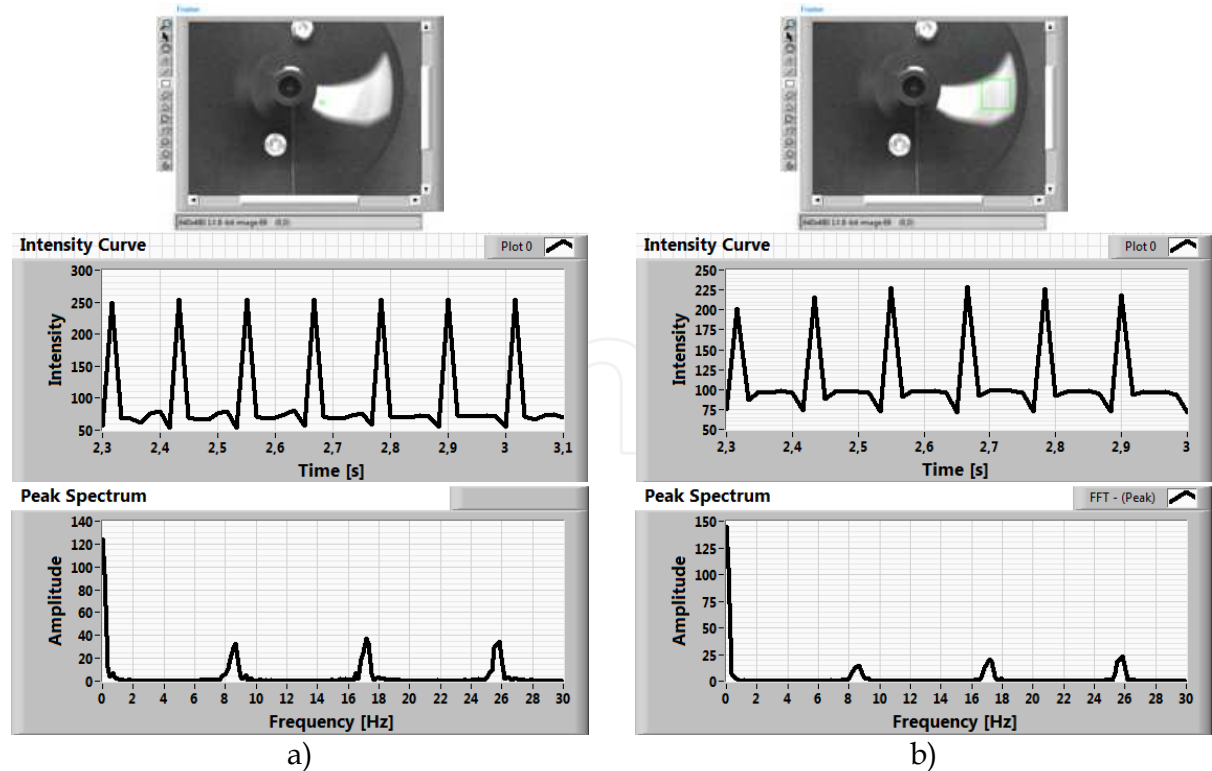


Fig. 17. a) Measurement 3: ~9 Hz / ROI size 5 x 5 (px) / dark background, b) Measurement 4: ~9 Hz / ROI size 45 x 45 (px) / dark background

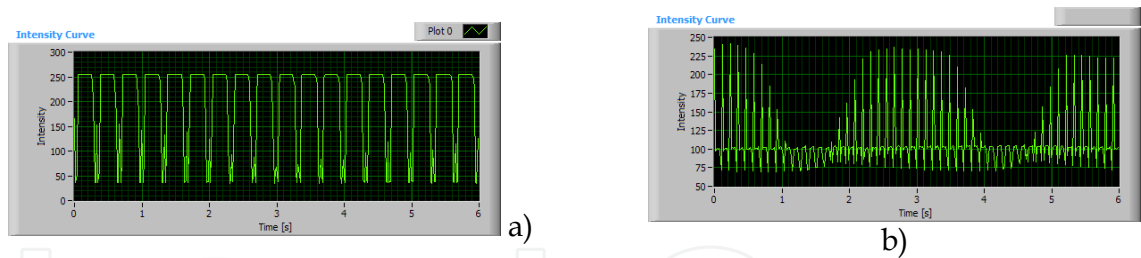


Fig. 18. a) Intensity variance curve for 3 Hz phantom without “floating”, b) Intensity variance curve for 9 Hz phantom with “floating”

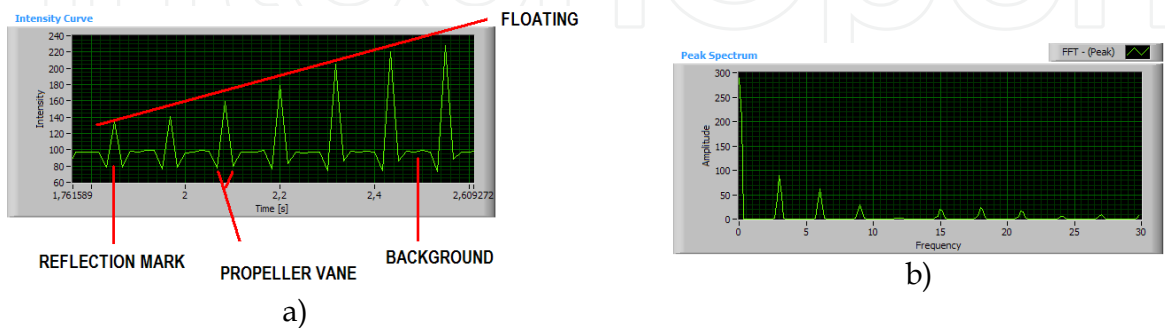


Fig. 19. a) Detailed show of intensity variance curve, b) Magnitude FFT spectrum for 3 Hz phantom

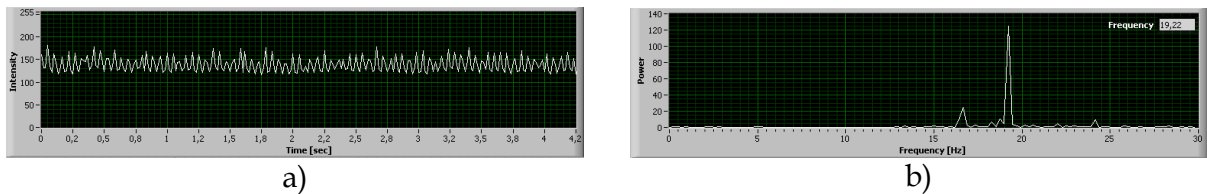


Fig. 20. a) Average ROI intensity variance graph, b) Power spectral density of variance graph

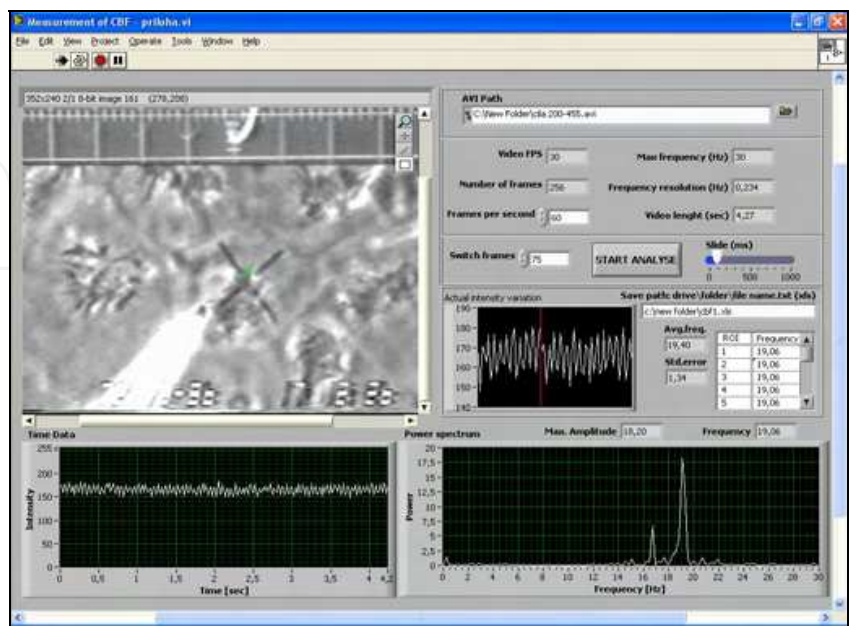


Fig. 21. CBF analysis Front Panel

LabVIEW contains components working with MS Office, so measurement results can be stored in Excel table. There is Front Panel of application for frequency analysis in Fig. 21. Second parameter – trajectory (or object position in the frame) is analysed by algorithms of object detection.

5.5 Analysis of cilia trajectory

The main tool in this phase of work is Pattern Matching. This tool searches a defined template on each frame of videosequence. Pattern Matching is a set of algorithms based on many techniques. The best known algorithm is cross correlation computing between an original image and a template. Computing of correlation consists of many elementary multiplications and it is very time-consuming; cross correlation cannot find rotated objects (rotation against the template max. 5 - 10°) and scaled objects (bigger or smaller than objects in the template) (NI, 2010). In practice we often use techniques working in frequency domain, pyramidal matching or other intelligent techniques. Pattern Matching and trajectory detection were tested on phantom videosequence with circular movement of the object. In Fig. 22, is shown the Front Panel of the application for trajectory detection. The Pattern Matching settings is shown in Fig. 23. The matching process is shown in Fig. 24 - Fig. 26. The frame to frame from videosequence is processing and trajectory and angle trajectory is calculated.

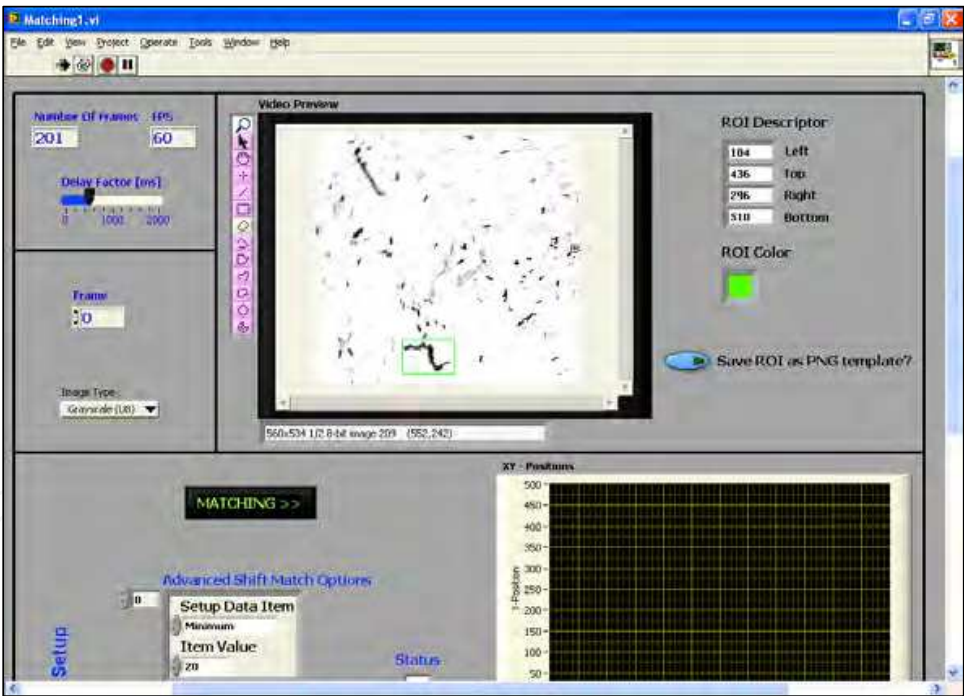


Fig. 22. Pattern Matching detection Front Panel

Designed workstation for high speed digital camera has several possibilities in many points of view partially mentioned above. Smart illumination lights created by LED modules are energy saving, directive sources with changeable emitting spectrums without need of cooling. This fact determinates usage of this hf digital microscopy not only for motion analysis of epithelial cilia. (This system was successfully used for analysis of small PCB traces.)

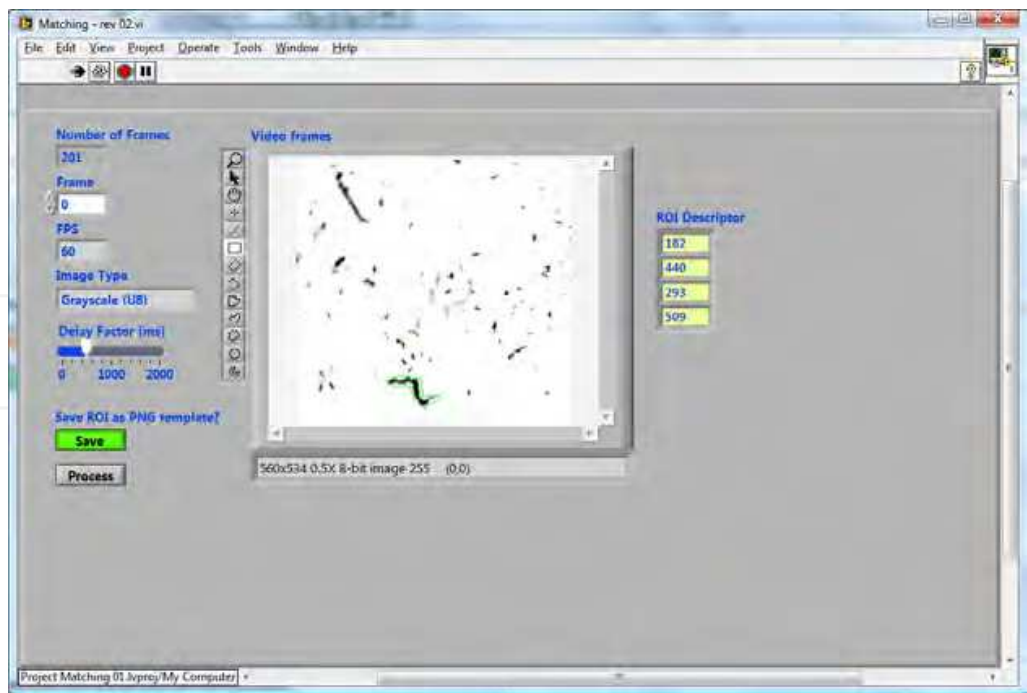


Fig. 23. Pattern Matching setting Front Panel

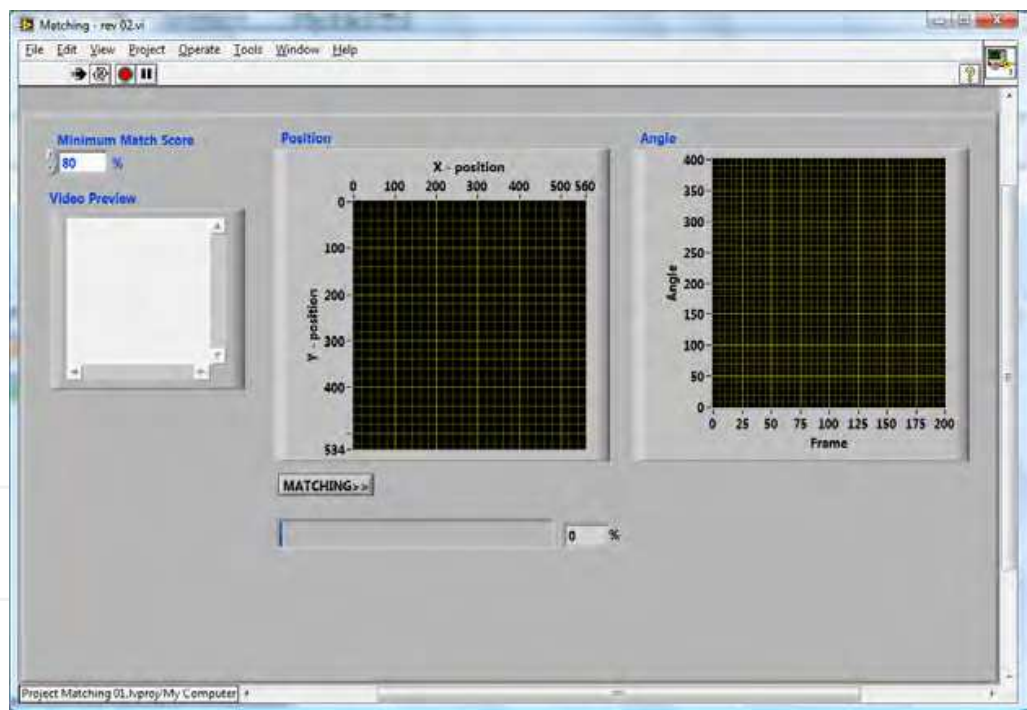


Fig. 24. Pattern Matching processing window “Matching Start”

Another possibilities result from LabVIEW Web Publishing tool usage. Acquisition computer with running virtual instruments is set as server and these scripts can be remote controlled from client computers linked through Ethernet / Internet network. Measurement can start e.g. in Martin hospital and recording or signal processing of recorded sequences can be fully controlled from Žilina or other cooperative clinics. But this remote control needs high speed Internet connection.

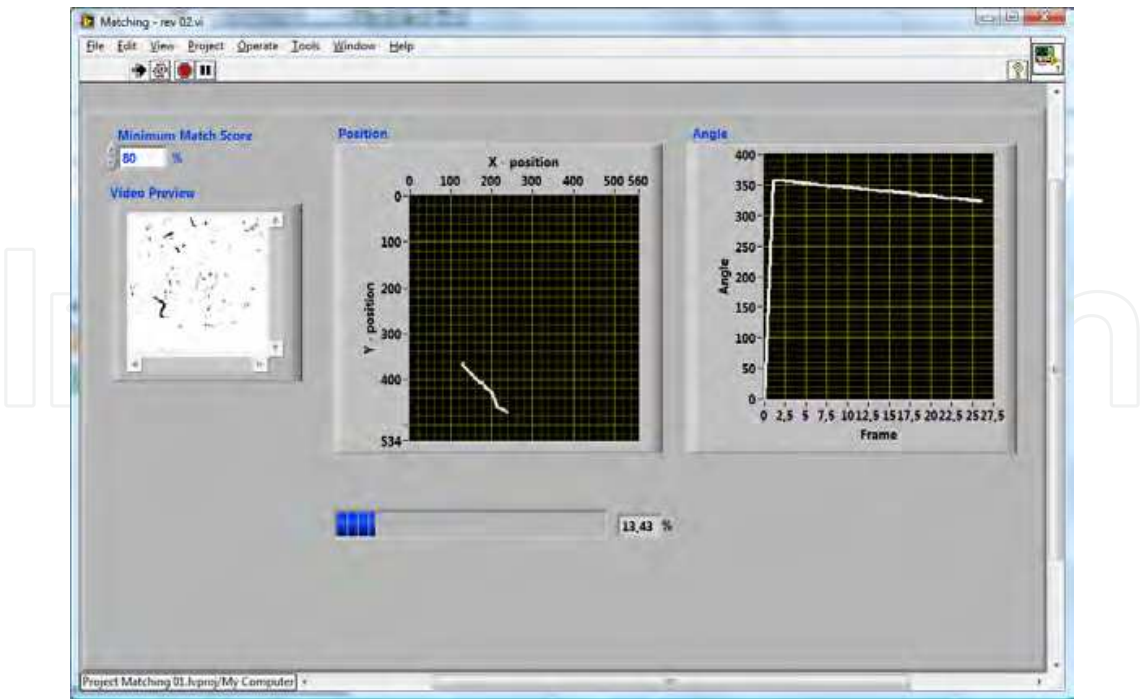


Fig. 25. Pattern Matching processing window – matching is in process (14%)

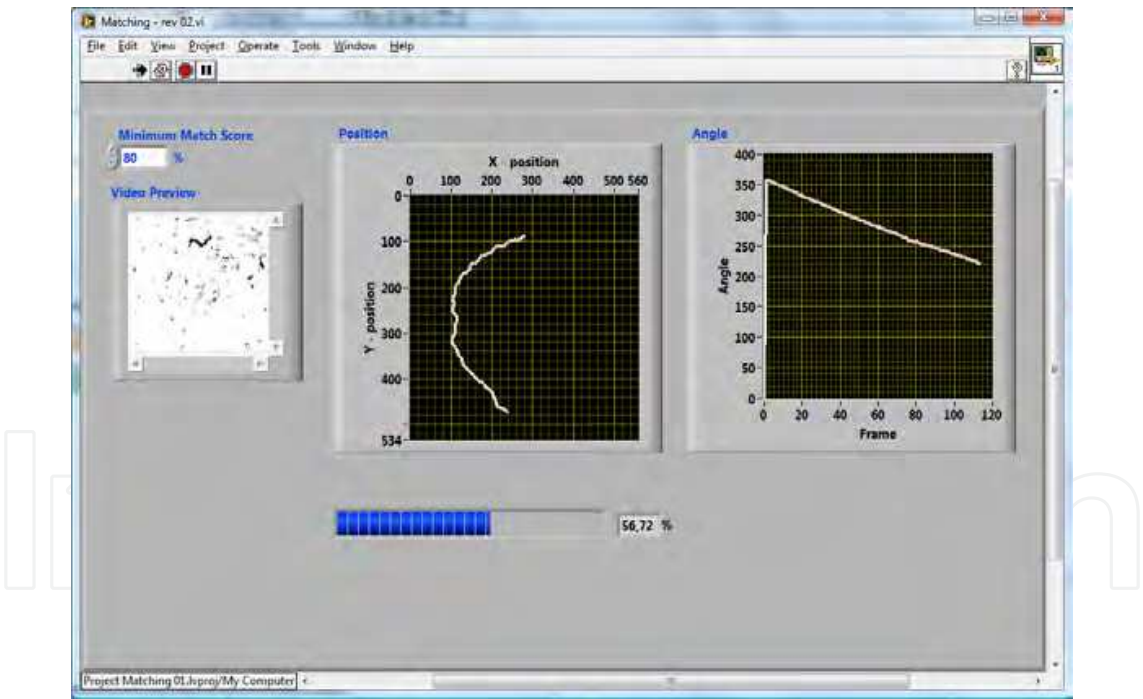


Fig. 26. Pattern Matching processing window – matching is in process (57%)

Acquisition computer is also via Ethernet connection linked with central server, where obtained video sequences are stored on hard drives in secured databases. LabVIEW analysis application generates Excel table (*.xls) with main analysis presets and results (Fig. 27a), which can be distributed on selected e-mail, server folder or directly to HIS (hospital / clinic information system). These LabVIEW tools for network communication speed up distributions of materials and results for analysis between cooperating clinics and institutes.

Video data and images from camera connected to light microscope can be projected from projector. In this mode specialists can do consilium and discuss about any problem. Measurement, results and discussions may be presented with help of suitable conference client. Our team in University of Žilina is testing Click to Meet client for online discussions and webminars, where logged users can share media files, images, documents and web pages, talk together through video and audio channel (Fig. 27b). This client runs on the same server (secured port 8080), where is clinical database with video sequences, applications and analysis results.

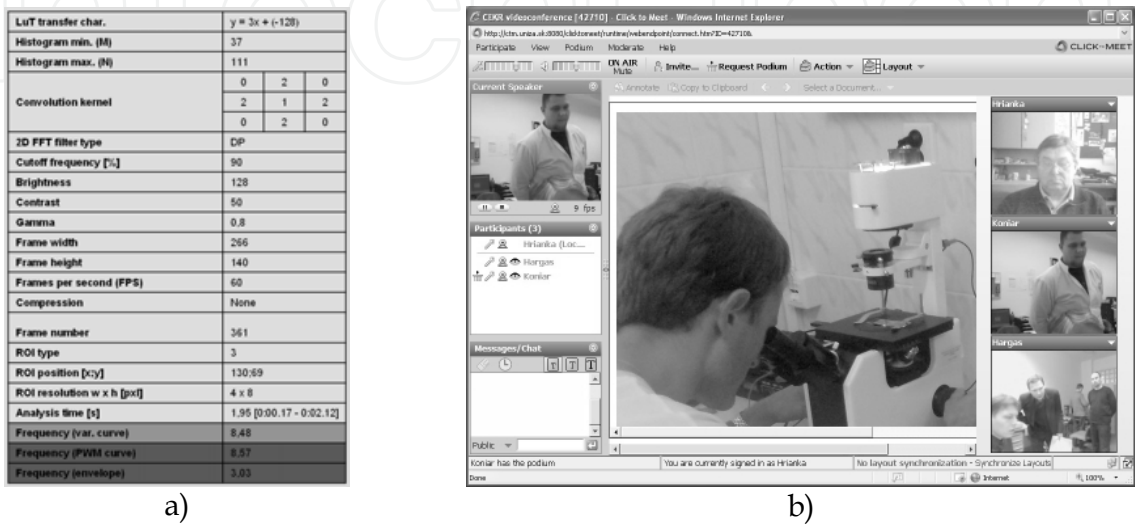


Fig. 27. a) Excel table generated in analysis LabVIEW application for given video sequence stored in server database / HIS analysis, b) Click to Meet conference client; discussion on experiment took in Jessenius medical faculty in Martin

6. Conclusion

In medical praxis – especially in diagnostics of respirathory apparatus – CBF represents very important parameter for describing various pathologies of epithelium. Designed solution for measuring object beating frequency from video sequence using tools of image analysis and spectral analysis simplifies present used methods and reduces usage of hardware devices. Using some development environment NI LabVIEW we can create fully automated application with interactive inputting of some parameters.

In the first approach, algorithms were tested on phantoms with defined frequency. Intensity variance curve analysis can be used in many other applications dedicated to frequency measurement not only in biological environment. Designed hardware acquisition system can be used with or without microscope in applications, where placement of kinematics parameters sensors is not able. Intelligent regulation of condenser illumination through image features extraction and histogram analysis enables fully automated approach to video sequence acquisition.

Biomedical solution of high speed camera workstation is composed from medical, power electronics, signal processing and telecommunications tasks. Software modules represented by LabVIEW enables remote control of experiments and offline analysis and do whole work more effective. Due to changeable modules and open architecture, it is easy to change any module and upgrade the workstation.

After a series of experimental measurements, system is ready for use in clinical environment (clinic of children and youth or institute of pharmacology). First clinical measurements will create useful feedback for technical support for final debugging of system parts.

7. Acknowledgment

Results of these experiments were made with support of grant agency VEGA, project No. 1/0320/10,, they are parts of project "Centre of Experimental and Clinical Respiriology", IMTS code: 26220120004, "Centre of Experimental and Clinical Respiriology II", IMTS code: 26220120034, "Measurement of Respiratory Epithelium Cilium Kinematics", IMTS code: 26220120019 funded by European Community, also for financial support to Slovak Research.

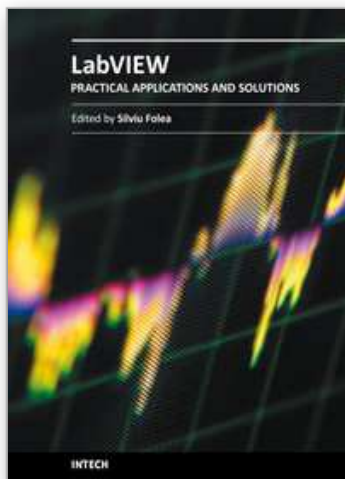


„We supported the research activities in Slovakia/Project is co-financed from EU sources“

8. References

- Brigham E. O. (1988): *The Fast Fourier Transform and Applications*, Prentice-Hall, ISBN: 0133075052, New York
- Chilvers M. A., O'Callaghan Ch. (2000): Analysis of ciliary beat pattern and beat frequency using digital high speed imaging: comparison with the photomultiplier and photodiode methods, *Thorax* 2000, Vol. 55, pp. 314-37, BMJ Publishing Group Ltd & British Thoracic Society (April)
- Drgoňa P. - Bobek V. - Dobrucký B. - Frivaldský M. (2009): Performance analysis of equation computation for real time model of PMSM for VHFIM control of PMSM position drive, *International Conference on ELECTRICAL DRIVES and POWER ELECTRONICS*, Dubrovnik, October 2009
- Duchoň, F., Štrenger, M. (2008): Microsoft Robotics Studio, *AT&P Journal Plus*, Vol. 10, No. 1, pp. 18-23., ISSN 1336-5010
- Eyman S. (2006): Ultrastructural Studies of the Airway Epithelium in Airway Diseases (Digital Comprehensive Summaries of Uppsala Dissertations from the Faculty of Medicine 123), *Acta Universitatis Upsaliensis*, ISBN 91-554-6492-0, Uppsala, 2006
- Frivaldsky M., Drgoňa P., Příkopová A. (2009): Design and modeling of 200kHz 1,5kW LLC power semiconductor resonant converter, *IEEE International conference on applied electronics*, Pilsen, September 2009
- Gheber L., Priel Z. (1997): Extraction of cilium beat parameters by the combined application of photoelectric measurements and computer simulation, *Biophysical Journal*, Vol. 72, No. 1, ISSN 1542-0086
- Jandoš F., Říman R., Gemperle A. (1985): *Využití moderních laboratorních metod v metalografii*, SNTL Praha (in Czech)
- Javorka, K. et al (2001): *Medical Physiology*, Osveta, ISBN 80-8063-023-2, Martin (in Slovak)

- Jelinek R. et al (2003): Histologie embryologie, In : *Charles University*, 16. 02. 2011, <http://old.lf3.cuni.cz/histologie/materialy/doc/skripta.pdf>
- National Instruments (2010): NI Vision Concepts Manual
- Špánik P., Frivaldsky M., Drgoňa P., Kandrác J. (2010): Efficiency increase of switched mode power supply trough optimization of transistor's commutation mode, *Electronics and electrical engineering*, No. 9 (105), pp. 49-52, ISSN 1392-1215
- Zhang, L., Sanderson, M. J. (2003): Oscillations in ciliary beat frequency and intracellular calcium concentration in rabbit tracheal epithelial cells induced by ATP, *The Journal of Physiology*, Vol. 546, No. 3, ISSN: 0022-3751



Practical Applications and Solutions Using LabVIEW™ Software

Edited by Dr. Silviu Folea

ISBN 978-953-307-650-8

Hard cover, 472 pages

Publisher InTech

Published online 01, August, 2011

Published in print edition August, 2011

The book consists of 21 chapters which present interesting applications implemented using the LabVIEW environment, belonging to several distinct fields such as engineering, fault diagnosis, medicine, remote access laboratory, internet communications, chemistry, physics, etc. The virtual instruments designed and implemented in LabVIEW provide the advantages of being more intuitive, of reducing the implementation time and of being portable. The audience for this book includes PhD students, researchers, engineers and professionals who are interested in finding out new tools developed using LabVIEW. Some chapters present interesting ideas and very detailed solutions which offer the immediate possibility of making fast innovations and of generating better products for the market. The effort made by all the scientists who contributed to editing this book was significant and as a result new and viable applications were presented.

How to reference

In order to correctly reference this scholarly work, feel free to copy and paste the following:

Libor Hargaš, Dušan Koniar and Stanislav Štofán (2011). Sophisticated Biomedical Tissue Measurement Using Image Analysis and Virtual Instrumentation, Practical Applications and Solutions Using LabVIEW™ Software, Dr. Silviu Folea (Ed.), ISBN: 978-953-307-650-8, InTech, Available from:

<http://www.intechopen.com/books/practical-applications-and-solutions-using-labview-software/sophisticated-biomedical-tissue-measurement-using-image-analysis-and-virtual-instrumentation>

INTECH
open science | open minds

InTech Europe

University Campus STeP Ri
Slavka Krautzeka 83/A
51000 Rijeka, Croatia
Phone: +385 (51) 770 447
Fax: +385 (51) 686 166
www.intechopen.com

InTech China

Unit 405, Office Block, Hotel Equatorial Shanghai
No.65, Yan An Road (West), Shanghai, 200040, China
中国上海市延安西路65号上海国际贵都大饭店办公楼405单元
Phone: +86-21-62489820
Fax: +86-21-62489821

© 2011 The Author(s). Licensee IntechOpen. This chapter is distributed under the terms of the [Creative Commons Attribution-NonCommercial-ShareAlike-3.0 License](https://creativecommons.org/licenses/by-nc-sa/3.0/), which permits use, distribution and reproduction for non-commercial purposes, provided the original is properly cited and derivative works building on this content are distributed under the same license.

IntechOpen

IntechOpen